Performance Enhancement Through Joint Detection of Cochannel Signals Using Diversity Arrays

Stephen J. Grant, *Student Member, IEEE,* and James K. Cavers, *Member, IEEE*

***Abstract*— Joint detection based on exploiting differences among the channels employed by several users allows a receiver to distinguish cochannel signals without reliance on spectrum spreading. This paper makes a number of new contributions to the topic: it provides an analytical expression for the union bound on average symbol-error rate for an arbitrary number of users and diversity antennas in a fading environment, for both perfect and imperfect channel state information (CSI), and it compares the performance of joint detection with diversity antennas against classical minimum-mean-square-error (MMSE) combining. The performance is remarkable. With accurate CSI, several users can experience good performance with only a single antenna; moreover, for perfect CSI, only a 2-dB penalty is incurred for each additional user. With several antennas, many more users than the number of antennas may be supported with a slow degradation in performance for each additional user. Furthermore, high accuracy is not required from the channel estimation process. In all cases, the performance of joint detection exceeds that of MMSE combining by orders of magnitude.**

***Index Terms*—Antenna arrays, cochannel interference, fading channels, multidimensional signal detection, multiuser channels.**

I. Introduction

JOINT detection is a method whereby the central receiver in a communication system exploits differences among several cochannel users' signals in order to make a simultaneous decision on all of the users' data. In this way, several signals can occupy the same frequency and time slot, leading to improved spectrum efficiency and system capacity.

Recently, much attention has been focused on joint detection in the context of code-division multiple-access (CDMA) systems, since the central receiver has knowledge of all users' orthogonal spreading sequences, which allows the signals to be distinguished. One of the most referenced works in this area is that by Verdu [1]. Subsequent works, e.g., [2] and [3], focused on the development of suboptimal detectors, since the computational complexity of the joint detection algorithm increases exponentially with the number of users—a potential problem for a CDMA system with many users.

An alternative method of distinguishing cochannel signals is to exploit differences in the channels between each user and the receiver. This method does not rely on spectrum spreading and it can, therefore, be applied to narrow-band systems, such as frequency-division multiple access (FDMA) or time-division multiple access (TDMA). Since the number of users sharing the same slot is likely to be much less than in a CDMA system, the computational complexity of the joint algorithm may not be a significant issue.

Joint detection based solely on channel differences has received only limited attention in the literature, e.g., [4]–[6]. In both [4] and [5] constant channels and perfect channel state information (CSI) are assumed, although in [4] multichannel reception is considered. In [6] deterministic channel estimation offsets are investigated, but the channel and the estimation errors are constant, and the receiver has only one channel available.

The present paper makes a number of new contributions. It appears to be the first to address multiuser detection based on channel differences in the context of fading channels. It provides an analytical expression for the union bound on average symbol-error rate for an arbitrary number of users and diversity antennas, and for both perfect and imperfect CSI. In addition, it compares the performance of joint detection with diversity antennas against minimum-mean-square-error (MMSE) antenna combining—a classical approach for suppressing cochannel interference when making single-user decisions [7]. Although the model has been simplified by requiring users to be synchronized by symbol, this study provides the motivation for investigation of asynchronous performance.

The results are striking. With accurate CSI, several users can experience good performance with only a single antenna. With a few antennas, many more users than antennas can be supported and the accuracy of the CSI can be quite lax. In all cases, joint detection outperforms MMSE combining by many decibels or orders of magnitude.

In Section II the system model is presented. In Section III the metric for the maximum-likelihood joint detection receiver is derived. In Section IV we derive an analytical expression for the average bit-error rate (BER) for the joint detection receiver and a quasi-analytical expression for BER for the MMSE combining receiver. Section V presents results highlighting the performance of joint detection and comparing it with MMSE combining. Finally, conclusions are drawn in Section VI.

II. System Model

The system considered in this paper concerns the transmission of M cochannel signals over frequency-flat Rayleigh-fading channels. The signals are assumed to be Q-ary phase-

Paper approved by K. B. Letaief, the Editor for Wireless Systems of the IEEE Communications Society. Manuscript received November 30, 1997; revised March 3, 1998. This work was supported by a postgraduate scholarship from the Natural Sciences and Engineering Research Council of Canada. This paper was presented in part at the 48th IEEE Vehicular Technology Conference, Ottawa, Ont., Canada, May 18–21, 1998.

The authors are with the School of Engineering Science, Simon Fraser University, Burnaby, B.C. V5A 1S6, Canada (e-mail: grantq@sfu.ca; cavers@sfu.ca).

Publisher Item Identifier S 0090-6778(98)05567-6.

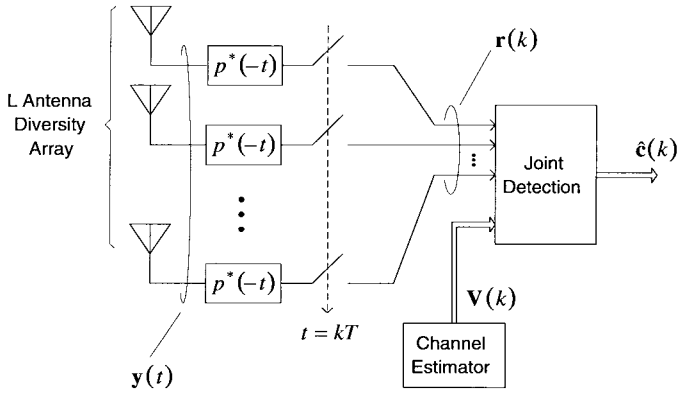

Fig. 1. Model of joint detection receiver.

shift keying (PSK) modulated and synchronized by symbol. L-fold antenna diversity is employed at the receiver with the antenna elements spaced far enough apart to ensure independent fading. A model of the receiver is shown in Fig. 1. A restriction is made to the symbol-synchronous case which allows an illustrative vector/matrix description of the system, leading to results that are easily interpreted and show the trends that would likely occur in a more typical asynchronous system.

Note that throughout this paper the following conventions are used: variables in italics are scalars, lowercase boldface variables are vectors, and uppercase boldface variables are matrices. Furthermore, † and ^{T} denote, respectively, the complex conjugate transpose and regular transpose of a vector or matrix, and * denotes complex conjugate. Since all signals are represented by their complex baseband equivalents, the power (or variance) of the bandpass signal $\tilde{v}(t)$, with baseband equivalent $v(t)$, is $P = \frac{1}{2}E[|v(t)|^2]$, where $E[\cdot]$ is the expectation operator.

Each user's transmitted signal is given by

$$s_m(t) = A_m \sum_k c_m(k)p(t - kT) \tag{1}$$

where $c_m(k)$ is the mth user's PSK data symbol during the kth signaling interval, normalized such that $|c_m(k)|^2 = 1$, $p(t)$ is a root Nyquist pulse normalized to unit energy, i.e., $\int_{-\infty}^{\infty} |p(t)|^2\,dt = 1$, T is the symbol period, and $A_m = \sqrt{2P_m}$, where P_m is the average power in $\tilde{s}_m(t)$.

The channels between the multiple users and multiple antennas are described by the channel gain matrix

$$\mathbf{G}(t) = \begin{bmatrix} g_{11}(t) & g_{12}(t) & \cdots & g_{1M}(t) \\ g_{21}(t) & g_{22}(t) & \cdots & g_{2M}(t) \\ \vdots & \vdots & \ddots & \vdots \\ g_{L1}(t) & g_{L2}(t) & \cdots & g_{LM}(t) \end{bmatrix} \tag{2}$$

where the zero-mean complex Gaussian random variable $g_{lm}(t)$ is the gain of the channel between the mth user and lth antenna. Due to independent fading across the antenna array, the L elements of the mth column of $\mathbf{G}(t)$, denoted by the channel gain vector $\mathbf{g}_m(t)$, are independent and are assumed to have equal variance $\sigma_{g_m}^2$. Furthermore, the users are assumed to be spaced far enough apart (a few wavelengths) that the columns of $\mathbf{G}(t)$ are mutually independent.

The output of the antenna array is the signal plus noise vector

$$\mathbf{y}(t) = \mathbf{G}(t)\mathbf{s}(t) + \mathbf{z}(t) = \sum_{m=1}^{M} \mathbf{g}_m(t)s_m(t) + \mathbf{z}(t) \tag{3}$$

where $\mathbf{s}(t)$ is the length-M vector of transmitted signals. The elements of the noise vector $\mathbf{z}(t)$ are independent white Gaussian noise processes with double-sided power spectral density N_o. Upon reception, $\mathbf{y}(t)$ is passed through a bank of matched filters each with impulse response $p^*(-t)$ and then sampled every T seconds to produce the vector

$$\mathbf{r}(k) = \sum_{m=1}^{M} A_m\mathbf{g}_m(k)c_m(k) + \mathbf{n}(k) \tag{4}$$

where the elements of $\mathbf{g}_m(k)$ and $\mathbf{n}(k)$ are zero mean with variance $\sigma_{g_m}^2$ and N_o, respectively. With reference to (4), the average per-branch signal-to-noise ratio (SNR) for user m at the input to the detector is defined as

$$\Gamma_m = \frac{\frac{1}{2}E[|A_m g_{lm}(k)c_m(k)|^2]}{\frac{1}{2}E[|n_l(k)|^2]} = \frac{A_m^2\sigma_{g_m}^2}{N_o}. \tag{5}$$

To aid detection, the channel estimator provides the receiver with estimates, denoted $\mathbf{V}(k)$, of the channel gain matrix. Consistent with previous notation, the channel estimate vector $\mathbf{v}_m(k)$ denotes the mth column of $\mathbf{V}(k)$. To keep the treatment general, we have not prescribed a specific channel estimation scheme, although the estimates are typically obtained through the use of embedded references such as pilot tones or pilot symbols [8].

After matched filtering, the received vector $\mathbf{r}(k)$ along with the channel estimates in $\mathbf{V}(k)$ are input to the detector, which makes a joint decision on all users' symbols using the metric derived in Section III. The output of the detector is the vector of symbol decisions $\hat{\mathbf{c}}(k)$, which is an estimate of the transmitted data vector $\mathbf{c}(k) = (c_1(k), c_2(k), \cdots, c_M(k))$.

III. Joint Detection Metric

Let $\{\mathbf{c}_i = (c_{i1}, c_{i2}, \cdots, c_{iM})\}$ be the set of all possible transmitted data vectors where the time dependence of all variables has been dropped in the subsequent analysis for convenience. For M users and a PSK constellation size of Q, the number of possible data vectors is Q^M. The joint detection metric is derived starting from the observation that the maximum *a posteriori* (MAP) detector selects that vector $\mathbf{c}_i$ from the set $\{\mathbf{c}_i\}$ for which the *a posteriori* probability $p(\mathbf{c}_i|\mathbf{r}, \mathbf{V})$ is maximum. Under the assumption of equiprobable data vectors, this is equivalent to maximizing the probability $p(\mathbf{r}|\mathbf{c}_i, \mathbf{V})$.

It is assumed in this study that the mth user's channel estimate $\mathbf{v}_m$ is a zero-mean complex Gaussian random vector correlated with the true channel gain vector $\mathbf{g}_m$. As with $\mathbf{g}_m$, it is assumed that the elements of $\mathbf{v}_m$ are independent and have equal variance $\sigma_{v_m}^2$. Furthermore, it is assumed that the correlation between $\mathbf{v}_m$ and $\mathbf{g}_m$ is described by the covariance matrix

$$\mathbf{R}_{\mathbf{g}_m,\mathbf{v}_m} = \tfrac{1}{2}E[\mathbf{g}_m\mathbf{v}_m^\dagger] = \rho_m\sigma_{g_m}\sigma_{v_m}\mathbf{I} \tag{6}$$

where ρ_m denotes the correlation coefficient between corresponding elements of $\mathbf{v}_m$ and $\mathbf{g}_m$, and $\mathbf{I}$ is the $L \times L$ identity matrix. Implicit in this assumption is that ρ_m is the same for all antennas and that v_{lm} on one antenna is uncorrelated with g_{lm} on a different antenna.

It is important to emphasize that the ρ_m's (generally complex quantities all with $|\rho_m| \leq 1$) collectively reflect the quality of channel estimation. For the limiting case of perfect CSI, ρ_m is equal to unity for all users. Note that in typical channel estimation schemes such as pilot-symbol-assisted modulation (PSAM) [8], ρ_m is expected to vary with SNR, tending to unity with very large SNR. This will be discussed in more detail in Section V-A.

Since $\mathbf{g}_m$ and $\mathbf{v}_m$ are jointly Gaussian with independent components, we can write

$$\mathbf{g}_m = \beta_m \mathbf{v}_m + \mathbf{e}_m \tag{7}$$

where $\beta_m = \rho_m \sigma_{g_m}/\sigma_{v_m}$ is the coefficient for MMSE estimation of $\mathbf{g}_m$ from $\mathbf{v}_m$ and, by the principle of orthogonality, the channel estimation error vector $\mathbf{e}_m$ is uncorrelated with $\mathbf{v}_m$. The conditional mean and covariance matrix of $\mathbf{g}_m$ are then

$$\boldsymbol{\mu}_{\mathbf{g}_m|\mathbf{v}_m} = \beta_m \mathbf{v}_m \tag{8a}$$

$$\mathbf{R}_{\mathbf{g}_m|\mathbf{v}_m} = \sigma_{e_m}^2 \mathbf{I} \tag{8b}$$

respectively. The estimation error variance is, in turn, given by

$$\sigma_{e_m}^2 = \sigma_{g_m}^2 - |\beta_m|^2 \sigma_{v_m}^2 = (1 - |\rho_m|^2)\sigma_{g_m}^2. \tag{9}$$

Note that in this paper $\mathbf{v}_m$ is scaled, for convenience, such that $|\beta_m| = 1$. Even with this magnitude normalization, β_m still occurs in subsequent equations since, in general, it is a complex quantity with an associated angle. The above equations clearly show that for perfect CSI from the channel estimator, $\sigma_{e_m}^2 = 0$ and $\mathbf{v}_m = \mathbf{g}_m$.

From (4), $\mathbf{r}$ conditioned on $\mathbf{c}_i$ and $\mathbf{V}$ is Gaussian. Use of (8a) and (8b) gives its conditional mean and covariance matrix, respectively, as

$$\boldsymbol{\mu}_{\mathbf{r}|\mathbf{c}_i,\mathbf{V}} = \sum_{m=1}^{M} A_m \beta_m c_{im} \mathbf{v}_m \tag{10a}$$

$$\mathbf{R}_{\mathbf{r}|\mathbf{c}_i,\mathbf{V}} = \left(\sum_{m=1}^{M} A_m^2 \sigma_{e_m}^2 + N_o \right) \mathbf{I}. \tag{10b}$$

The probability density function (pdf) of $\mathbf{r}$, conditioned on $\mathbf{c}_i$ and $\mathbf{V}$, can now be written as

$$p(\mathbf{r}|\mathbf{c}_i, \mathbf{V}) = \frac{1}{(2\pi)^L \left(\sum_{m=1}^{M} A_m^2 \sigma_{e_m}^2 + N_o \right)^L} \cdot \exp\left[-\frac{1}{2} \frac{\sum_{l=1}^{L} \left| r_l - \sum_{m=1}^{M} A_m \beta_m c_{im} v_{lm} \right|^2}{\sum_{m=1}^{M} A_m^2 \sigma_{e_m}^2 + N_o} \right]. \tag{11}$$

Neglecting hypothesis-independent terms, the appropriate joint detection metric to be minimized is

$$\Lambda_i = \sum_{l=1}^{L} \left| r_l - \sum_{m=1}^{M} A_m \beta_m c_{im} v_{lm} \right|^2. \tag{12}$$

Evidently, the receiver requires knowledge of the product $A_m v_{lm}$ for every user. Fortunately, this quantity is generated explicitly in a pilot-based channel estimator. The other required parameter β_m is determined at design time; however, if the true channel statistics differ from the design statistics, a bias is introduced. We have assumed the bias to be zero and focused the analysis on the random channel estimation errors.

It is interesting to note that for a single user, the metric defined in (12) leads to the well-known maximal-ratio-combining (MRC) receiver. For $M = 1$, after neglecting hypothesis independent terms, (12) reduces to

$$\Lambda_i = \mathrm{Re}\left[c_i^* \sum_{l=1}^{L} r_l v_l^* \right]. \tag{13}$$

Evidently, the receiver weights each antenna signal r_l by v_l^*, combines the L signals, and derotates the sum by the various symbol hypotheses to determine the most likely transmitted symbol.

IV. Error Probability Analysis

Section IV-A contains an analysis of the error performance of joint detection based on the metric derived above. For reference, Section IV-B contains an analysis of the error performance of the well-known MMSE combining receiver [7] with the addition of channel estimates. In contrast to joint detection, which exploits the CSI from other users to make a single joint decision, the MMSE combining receiver makes separate decisions on each user's symbol while attempting to suppress the interference from other users.

A. Joint Detection

Here we determine an upper bound on the probability of symbol error for user m, denoted P_{s_m}. First, let the transmitted data vector be $\mathbf{c}_j = (c_{j1}, c_{j2}, \cdots, c_{jM})$. According to (12), the detector chooses the erroneous data vector $\mathbf{c}_i = (c_{i1}, c_{i2}, \cdots, c_{iM})$ over $\mathbf{c}_j$ if $\Lambda_i < \Lambda_j$. The probability of this pairwise error event is denoted $P(D_{ij} < 0|\mathbf{c}_j)$, where $D_{ij} = \Lambda_i - \Lambda_j$.

The union bound on the probability of symbol error for user m, given that $\mathbf{c}_j$ is transmitted, is given by the sum of the pairwise error probabilities over the subset of vectors in $\{\mathbf{c}_i\}$ that differ in their mth position from $\mathbf{c}_j$. Assuming equiprobable transmitted data vectors and noting that the probability of error does not depend on which data vector is actually transmitted, we have

$$P_{s_m} \leq \sum_{i} P(D_{ij} < 0|\mathbf{c}_j) \tag{14}$$

where i indexes the subset of vectors in $\{\mathbf{c}_i\}$ that differ in their mth position from $\mathbf{c}_j$.

The pairwise error probability is determined in the following manner. First, using an alternative form of the metric defined in (12), the random variable D_{ij} can be written as a sum of L Hermitian quadratic forms

$$D_{ij} = \sum_{l=1}^{L} \mathbf{z}_l^{\dagger} \mathbf{F}_{ij} \mathbf{z}_l \tag{15}$$

where the length-$M+1$ vector $\mathbf{z}_l$ is defined as

$$\mathbf{z}_l = (r_l, v_{l1}, v_{l2}, \cdots, v_{lM})^T. \tag{16}$$

The Hermitian matrix $\mathbf{F}_{ij}$ is defined as

$$\mathbf{F}_{ij} = (\mathbf{u}_i \mathbf{u}_i^{\dagger} - \mathbf{u}_j \mathbf{u}_j^{\dagger})^* \tag{17}$$

where the vectors $\mathbf{u}_i$ and $\mathbf{u}_j$ are given by

$$\mathbf{u}_i = (1, -A_1\beta_1 c_{i1}, -A_2\beta_2 c_{i2}, \cdots, -A_M\beta_M c_{iM})^T \tag{18a}$$

$$\mathbf{u}_j = (1, -A_1\beta_1 c_{j1}, -A_2\beta_2 c_{j2}, \cdots, -A_M\beta_M c_{jM})^T \tag{18b}$$

Next, observing (15), define the random variable $d_{ijl} = \mathbf{z}_l^{\dagger} \mathbf{F}_{ij} \mathbf{z}_l$. Since d_{ijl} is a Hermitian quadratic form in $M+1$ zero-mean complex Gaussian random variates, according to [9, eq. (B-3-21)] the two-sided Laplace transform of the pdf of d_{ijl} is

$$\phi_{d_{ijl}}(s) = \frac{1}{\det(\mathbf{I} + 2s\mathbf{R}\mathbf{F}_{ij})} \tag{19}$$

where the covariance matrix $\mathbf{R} = \frac{1}{2} E[\mathbf{z}_l \mathbf{z}_l^{\dagger} | \mathbf{c}_j]$ is given in (20), shown at the bottom of the page. The region of convergence of $\phi_{d_{ijl}}(s)$ is the vertical strip enclosing the $j\omega$ axis bounded by the closest pole on either side. Due to independent fading across the antenna array, the $\mathbf{z}_l$'s in (15) are independent as are the d_{ijl}'s. Consequently, the two-sided Laplace transform of the pdf of $D_{ij} = \sum_l d_{ijl}$ is simply the product $\Phi_{D_{ij}}(s) = \prod_l \phi_{d_{ijl}}(s)$. Moreover, since $\mathbf{R}$ is independent of l

$$\Phi_{D_{ij}}(s) = \left[\frac{1}{\det(\mathbf{I} + 2s\mathbf{R}\mathbf{F}_{ij})} \right]^L \tag{21a}$$

$$= \left[\frac{1}{\prod_{k=1}^{M+1} (1 + s\lambda_{ijk})} \right]^L \tag{21b}$$

where λ_{ijk} is the kth eigenvalue of $2\mathbf{R}\mathbf{F}_{ij}$.

The inversion of (21b) is made easier by the fact that the matrix $2\mathbf{R}\mathbf{F}_{ij}$ has only two nonzero eigenvalues denoted λ_{ij1} and λ_{ij2} (see Appendix). Thus, rearranging (21b)

$$\Phi_{D_{ij}}(s) = \left[\frac{p_{ij1} p_{ij2}}{(s - p_{ij1})(s - p_{ij2})} \right]^L \tag{22}$$

where the convention is used that the pole $p_{ij1} = -1/\lambda_{ij1}$ is in the left half-plane, and the pole $p_{ij2} = -1/\lambda_{ij2}$ is in the right half-plane. Since (22) is similar in form to [10, eq. (4B.7)], suitable modifications give the sought-after pairwise error probability as

$$P(D_{ij} < 0 | \mathbf{c}_j) = \frac{1}{\left(1 - \frac{p_{ij2}}{p_{ij1}}\right)^{2L-1}} \sum_{k=0}^{L-1} \binom{2L-1}{k} \left(-\frac{p_{ij2}}{p_{ij1}}\right)^k. \tag{23}$$

Finally, by substituting this expression into (14), the union bound on the probability of error for user m is given by

$$P_{s_m} \le \sum_i \frac{1}{\left(1 - \frac{p_{ij2}}{p_{ij1}}\right)^{2L-1}} \sum_{k=0}^{L-1} \binom{2L-1}{k} \left(-\frac{p_{ij2}}{p_{ij1}}\right)^k \tag{24}$$

where, again, i indexes all those vectors in $\{\mathbf{c}_i\}$ that differ in their mth position from the transmitted vector $\mathbf{c}_j$.

For the special case of a single user, binary PSK (BPSK) signaling, and perfect CSI, (24) reduces to the result for the exact probability of bit error (rather than the union bound) for the MRC receiver. Since $M = 1$, the matrix $2\mathbf{R}\mathbf{F}_{ij}$ is only 2×2; therefore, its eigenvalues can be found analytically resulting in the pole ratio $r = p_2/p_1$ given by

$$r = \frac{1 + \sqrt{1 + \Gamma^{-1}}}{1 - \sqrt{1 + \Gamma^{-1}}} \tag{25}$$

where Γ is the average per-branch SNR defined in (5). The probability of bit error is then

$$P_b = \frac{1}{(1-r)^{2L-1}} \sum_{k=0}^{L-1} \binom{2L-1}{k} (-r)^k \tag{26}$$

which is equivalent to [10, eq. (7.4.15)].

$$\mathbf{R} = \begin{bmatrix} \sum_{m=1}^{M} A_m^2 \sigma_{g_m}^2 + N_o & A_1\beta_1\sigma_{v1}^2 c_{j1} & A_2\beta_2\sigma_{v2}^2 c_{j2} & \cdots & A_M\beta_M\sigma_{vM}^2 c_{jM} \\ A_1\beta_1^*\sigma_{v1}^2 c_{j1}^* & \sigma_{v1}^2 & 0 & \cdots & 0 \\ A_2\beta_2^*\sigma_{v2}^2 c_{j2}^* & 0 & \sigma_{v2}^2 & \cdots & 0 \\ \vdots & \vdots & \vdots & \ddots & \vdots \\ A_M\beta_M^*\sigma_{vM}^2 c_{jM}^* & 0 & 0 & \cdots & \sigma_{vM}^2 \end{bmatrix} \tag{20}$$

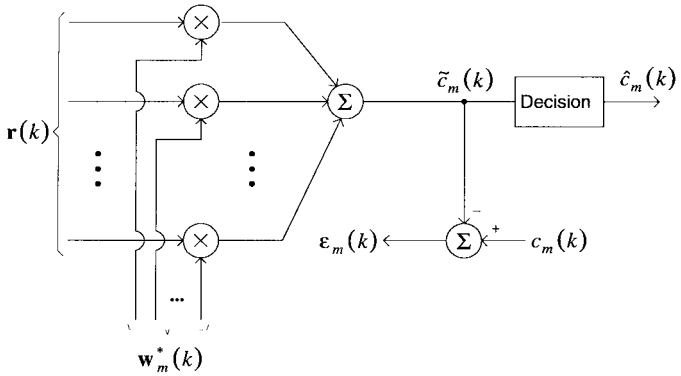

Fig. 2. Model of MMSE combining reciever for the mth user.

B. MMSE Combining

Here a quasi-analytical expression for the bit-error probability of the MMSE combining receiver (Fig. 2) using channel estimates is derived. For each individual user, the weight vector $\mathbf{w}_m(k)$ is chosen to minimize the mean-squared value of the error signal $\varepsilon_m(k) = c_m(k) - \tilde{c}_m(k)$ given by

$$\overline{\varepsilon}_m = \tfrac{1}{2} E[|c_m - \mathbf{w}_m^\dagger \mathbf{r}|^2 | c_m, \mathbf{V}] \tag{27}$$

where the time dependence has been dropped for convenience. Note that the expectation in (27) is taken over the joint ensemble of channel estimation errors, noise, and the $M-1$ interfering users' symbols. The output of the detector is the symbol decision $\hat{c}_m(k)$, which is chosen to be that symbol closest in Euclidean distance to the combiner output $\tilde{c}_m(k)$.

The optimal weight vector for the mth user is found by expanding (27), differentiating with respect to $\mathbf{w}_m$, setting the result to zero, and solving for $\mathbf{w}_m$. For the case of PSK modulation, the result is

$$\mathbf{w}_m^{opt} = (E[\mathbf{r}\mathbf{r}^\dagger | c_m, \mathbf{V}])^{-1} c_m^* E[\mathbf{r} | c_m, \mathbf{V}] \tag{28a}$$

$$= \left(\sum_{n=1}^{M} A_n^2 (\mathbf{v}_n \mathbf{v}_n^\dagger + 2\sigma_{e_n}^2 \mathbf{I}) + 2N_o \mathbf{I} \right)^{-1} A_m \beta_m \mathbf{v}_m \tag{28b}$$

where, to avoid confusion later, the subscript n is used in all summations. Equation (28b) generalizes the weight equation derived in [7] to include the case of imperfect channel estimation. For the special case of perfect channel estimation ($\sigma_{e_m}^2 = 0$ and $\mathbf{v}_m = \mathbf{g}_m$) (28b) and [7, eq. (9)], are equivalent.

For the case of BPSK modulation, the probability of bit error for the mth user, denoted P_{b_m} is

$$P_{b_m} = P[\mathrm{Re}[\tilde{c}_m] < 0 | c_m = +1]. \tag{29}$$

Unfortunately, the pdf of $\tilde{c}_m$ is difficult to obtain for $M > 1$ due to the matrix inversion in (28b). Thus, in order to determine BER's for arbitrary M, simulation is required. For $M = 1$, though, it can be shown that by using the matrix inversion lemma [11], (28b) reduces to the weight vector for the MRC receiver with bit-error probability given by (26).

Before resorting to simulation, some progress can be made toward a quasi-analytical BER expression by recognizing that the pdf of the random variable $\tilde{c}_m$ conditioned on both the channel estimate matrix $\mathbf{V}$, and the symbol vector $\mathbf{c} = (c_1, c_2, \cdots, c_M)$ is Gaussian. To see this, let $\tilde{c}_m = \mathbf{w}_m^\dagger \mathbf{r} = y + z$ where, using (4) and (7)

$$y = \mathbf{w}_m^\dagger \sum_{n=1}^{M} A_n \beta_n \mathbf{v}_n c_n \tag{30}$$

$$z = \mathbf{w}_m^\dagger \left(\sum_{n=1}^{M} A_n \mathbf{e}_n c_n + \mathbf{n} \right). \tag{31}$$

Observing (28b), $\mathbf{w}_m$ is deterministic for a given $\mathbf{V}$. Thus, for a given $\mathbf{c}$, y is deterministic as well, and z is Gaussian since both $\mathbf{e}_m$ and $\mathbf{n}$ are Gaussian. Furthermore, z is zero-mean. Therefore, given $\mathbf{c}$ with $c_m = +1$ and $\mathbf{V}$, the conditional probability of error is the probability that the real part of $\tilde{c}_m$ goes negative, given by

$$P[\mathrm{Re}[\tilde{c}_m] < 0 | \mathbf{c}, \mathbf{V}] = Q\left(\frac{\mathrm{Re}[y]}{\sigma_z} \right) \tag{32}$$

where $Q(\cdot)$ is the Gaussian Q-function, and the variance of z is given by

$$\sigma_z^2 = \left(\sum_{n=1}^{M} A_n^2 \sigma_{e_n}^2 + N_o \right) \mathbf{w}_m^\dagger \mathbf{w}_m. \tag{33}$$

The average probability of bit error for user m follows by substituting (30) and (33) in (32) and taking the expectation over the joint ensemble of the channel estimates and the interfering users' symbols

$$P_{b_m} = E\left[Q\left(\frac{\mathrm{Re}\left[\mathbf{w}_m^\dagger \sum_{n=1}^{M} A_n \beta_n \mathbf{v}_n c_n \right]}{\sqrt{\left(\sum_{n=1}^{M} A_n^2 \sigma_{e_n}^2 + N_o \right) \mathbf{w}_m^\dagger \mathbf{w}_m}} \right) \right] \tag{34}$$

where it is understood that $c_m = +1$. In this way, we have increased the simulation accuracy by performing the average over the noise and channel estimation error ensembles analytically.

Using (34), the BER for user m is determined through simulation by the following method: at each iteration generate an $L \times M$ matrix $\mathbf{V}$ of independent zero-mean complex Gaussian random samples, with the elements in column m having variance $\sigma_{v_m}^2$, calculate the weight vector $\mathbf{w}_m$ using (28b) along with (9), and then average the Q-function in (34) over all possible $\mathbf{c}$'s with $c_m = +1$.

V. Performance Results

In this section we provide some numerical results that follow from the analysis in Section IV. Specifically, the results highlight the performance of the following: 1) joint detection of equipower signals with a single antenna; 2) joint detection of equipower signals compared to MMSE combining for multiple antennas; and 3) joint detection of nonequipower users. In all cases both perfect and imperfect CSI are considered.

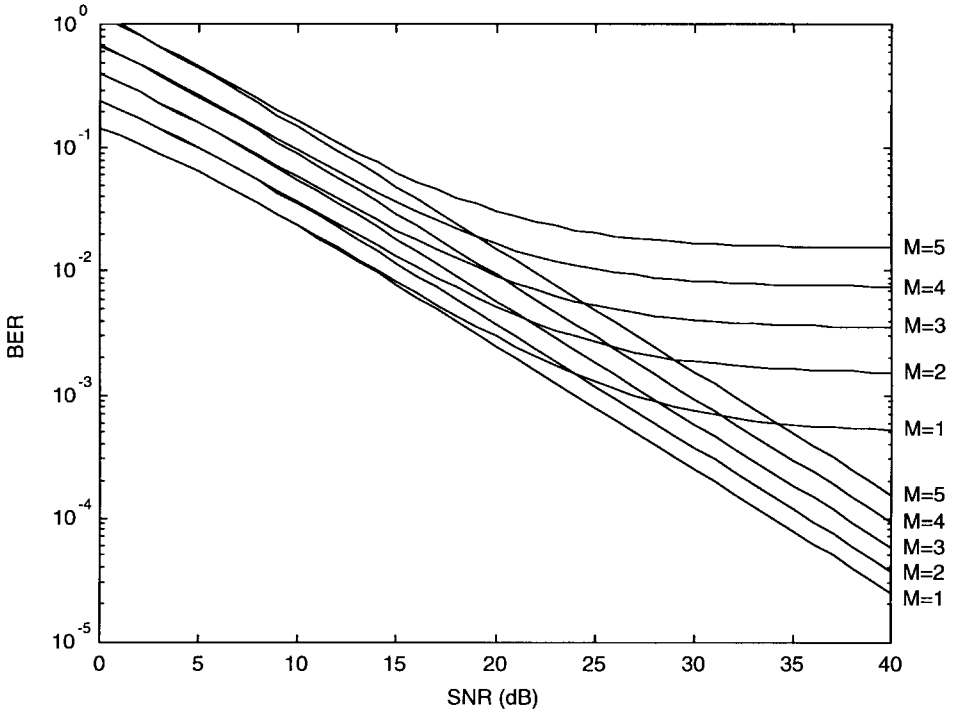

Fig. 3. Performance of joint detection of equipower users with a single antenna. The lower set of curves is for perfect CSI; the upper set is for imperfect CSI with $\rho_m = 0.999$ for all users.

Although the analysis in Section IV applies to Q-ary PSK in general, for simplicity, we limit the results in this section to the case of BPSK modulation ($Q = 2$). As discussed previously, perfect CSI is modeled by setting the channel estimation correlation coefficient ρ_m for all M users to unity; values of ρ_m less than unity imply imperfect CSI with estimation error variance $\sigma^2_{e_m}$ given by (9). For convenience, the channel gain variance $\sigma^2_{g_m}$ is set to 1/2 for all users so that the channels do not alter the power of the transmitted signals, and the per-branch SNR for user m defined in (5) becomes $\Gamma_m = P_m/N_o$. In this way, different receive powers for each user are modeled by assigning appropriate values to the P_m's.

A. Single Antenna

Fig. 3 shows the performance of joint detection of equipower signals using single antenna for both perfect and imperfect CSI; for the case of imperfect CSI, ρ_m is set to 0.999 for all users. Note that the performance of each user is identical since all signals are received at the same power level and ρ_m is the same for each user. With reference to the perfect CSI curves, it can be seen that the performance degrades by only about 2 dB for each additional user. This value decreases to approximately 0.2 dB with four antennas. In the low-SNR region the two sets of curves are coincident, implying that noise, rather than channel estimation error, is the dominant effect determining error rate; that is, $N_o \gg \sigma^2_{e_m}$ in this region. In contrast, in the high-SNR region, channel estimation error dominates the performance, causing an irreducible error rate similar to that observed in systems employing differential detection. As can be seen, though, up to four users may be supported while still maintaining an error rate below 10^{-2}—a striking result for only a single antenna.

Although these analytical results are for BPSK, Q-ary PSK ($Q = 4$) shows a similar behavior: the BER curves are parallel, with a degradation of about 4.8 dB for each additional user. This latter result was determined by simulation of Q-ary PSK with perfect CSI.

Our analytical results are quite general in that we have assumed an arbitrary—but fixed—ρ_m with no reference to the actual channel estimation scheme used. In a typical single-channel system employing PSAM [8], though, the channel estimation error variance $\sigma^2_{e_m}$ varies inversely with SNR over a wide range, i.e., $\sigma^2_{e_m} = b/\Gamma_m$. The constant of proportionality b depends on various parameters of the PSAM scheme such as interpolator order, pilot symbol spacing, and the Doppler fade rate. $\sigma^2_{e_m}$ is related to ρ_m through (9); thus, the variation of ρ_m with SNR can be modeled as $|\rho_m(\Gamma_m)| = \sqrt{1 - (b/\sigma^2_{g_m}\Gamma_m)}$.

For illustrative purposes, we present results using this model for ρ_m assuming a 1% Doppler fade rate, an 11th-order interpolator, and a pilot spacing of ten symbols ($b = 0.1613$). Fig. 4 compares the performance using the fixed and variable ρ_m models for the detection of $M = 4$ equipower users. A fixed ρ_m of 0.999 for all users is chosen for comparison since $\rho_m(\Gamma_m) \approx 0.999$ at the midpoint (20 dB) of the SNR range considered. As might be expected, the consequences of fixing ρ_m are that the error rate is pessimistic in the high-SNR region and somewhat optimistic in the low-SNR region. Using the variable ρ_m model, the error floor disappears since $\rho_m(\Gamma_m) \approx 1$ in the high-SNR region. In the low-SNR region the performance is degraded by approximately 2.5 dB. Moreover, the variable ρ_m curve runs essentially parallel to the perfect CSI curve with a performance degradation of approximately 2.5 dB. This behavior is typical of what we

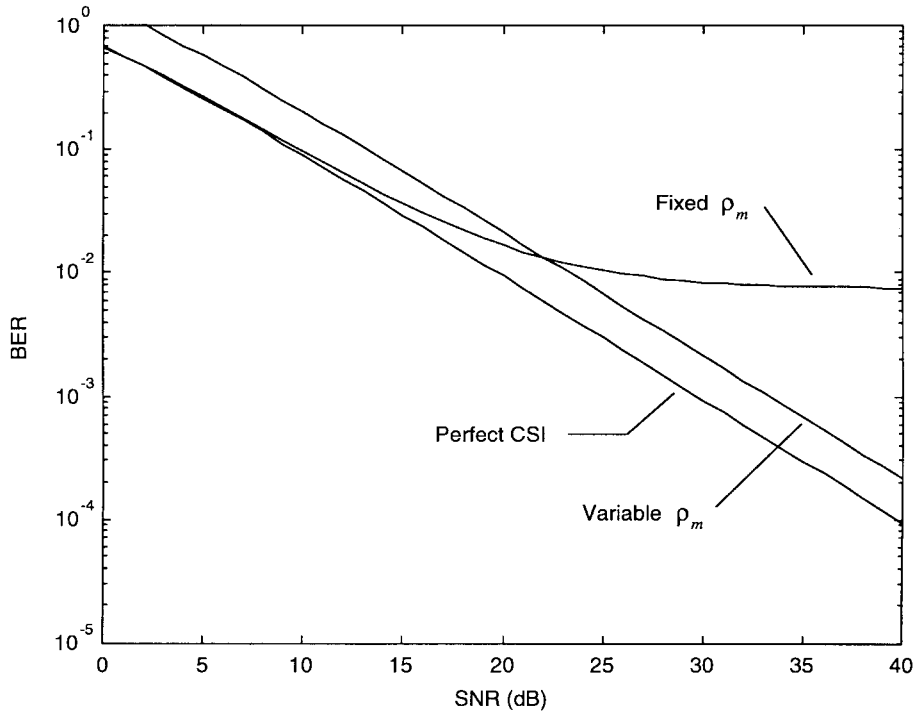

Fig. 4. Comparison of fixed and variable ρ_m models for the joint detection of $M = 4$ equipower users with a single antenna (fixed ρ_m is 0.999 for all users).

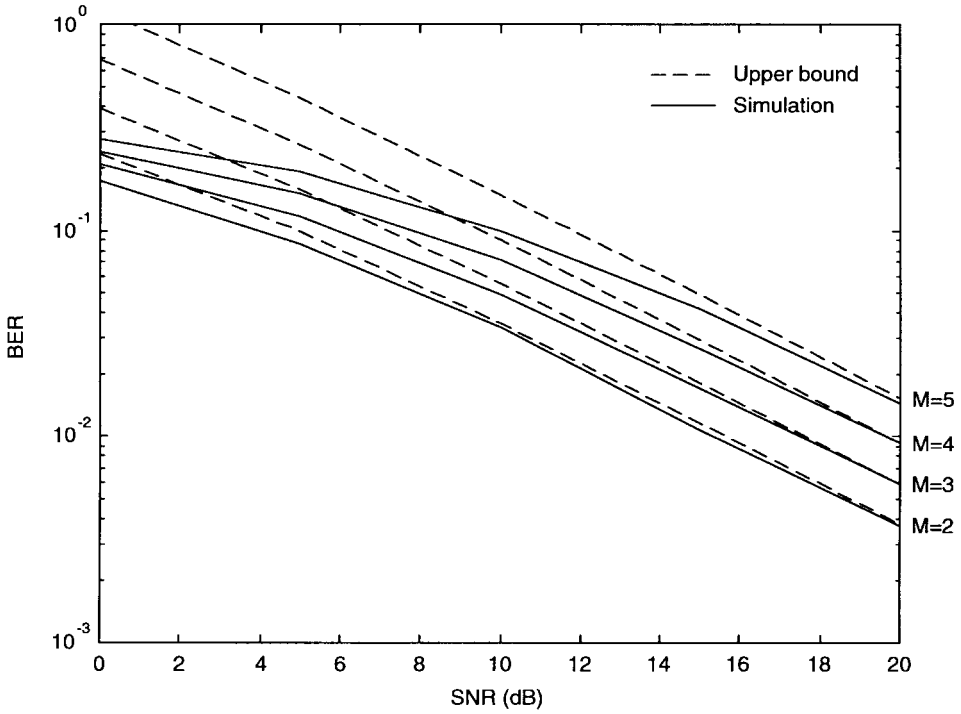

Fig. 5. Tightness of upper bound on BER for the joint detection of equipower users with a single antenna and perfect CSI.

have observed in other situations. We will return to modeling the variation of ρ_m with SNR in Section V-C. Until then, the fixed ρ_m model will be used for generality.

We also investigated tightness of the upper bound. Fig. 5, which compares the bound to simulation values for perfect CSI, shows that it is asymptotically tight with increasing SNR. As the number of users M increases, a given accuracy of the bound requires a somewhat higher SNR; however, the accuracy is quite satisfactory for normal values of BER. As for increasing the number of constellation points Q, the bound becomes loose, like the union bound for Q-ary PSK in conventional single-user operation; however, in such cases a better approximation can be obtained by considering only the dominant error events.

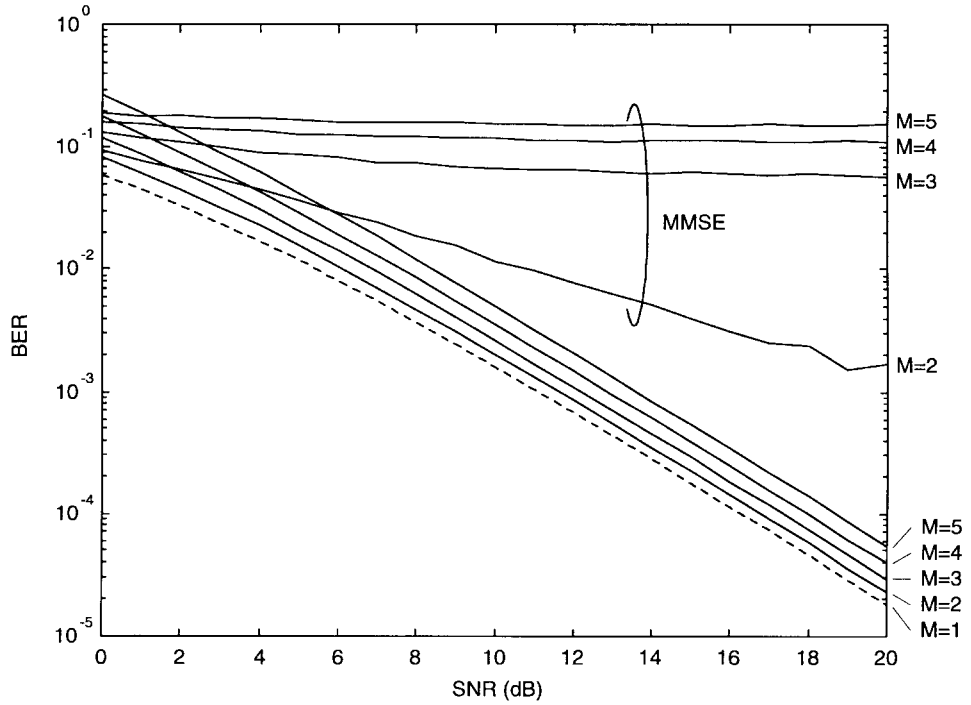

Fig. 6. Comparison of joint detection and MMSE combining with $L = 2$ antennas, equipower users, and perfect CSI.

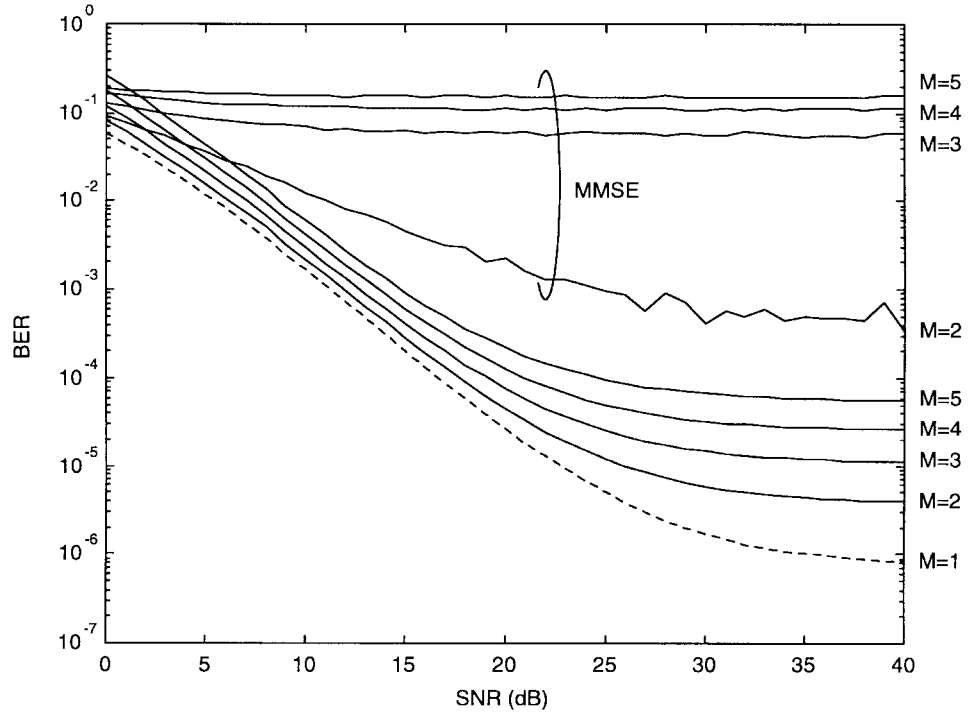

Fig. 7. Comparison of joint detection and MMSE combining with $L = 2$ antennas, equipower users, and imperfect CSI ($\rho_m = 0.999$ for all users).

B. Multiple Antennas

Fig. 6 shows the performance of joint detection of equipower signals compared to MMSE combining for $L = 2$ antennas and perfect CSI; Fig. 7 is for imperfect CSI with $\rho_m = 0.999$ for all users. Clearly, joint detection outperforms MMSE combining by a very large margin. Whereas for MMSE combining the performance is unacceptable when the number of users exceeds the number of antennas, the performance of joint detection degrades gracefully with each additional user. Note that if the variable ρ_m model is used, a similar effect to that observed in Fig. 4 occurs. That is, the joint detection curves in Fig. 7 become essentially parallel to those for the perfect CSI case, but shifted to the right by approximately 2 dB for $M = 2$ and 4 dB for $M = 5$. In contrast, the MMSE

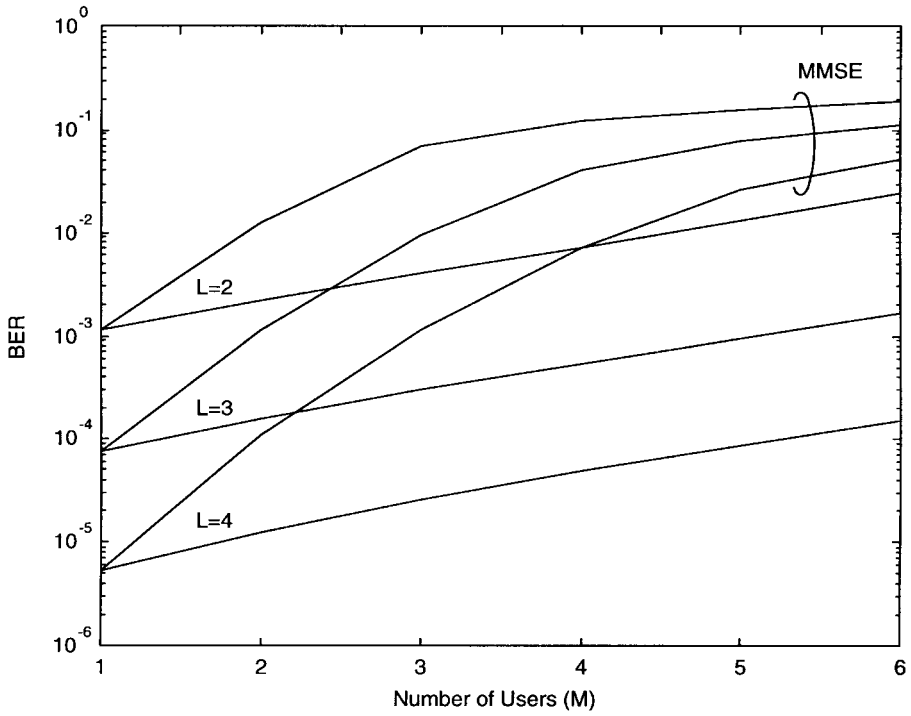

Fig. 8. Comparison of joint detection and MMSE combining at a fixed SNR of 12 dB with equipower users and imperfect CSI ($\rho_m = 0.999$ for all users).

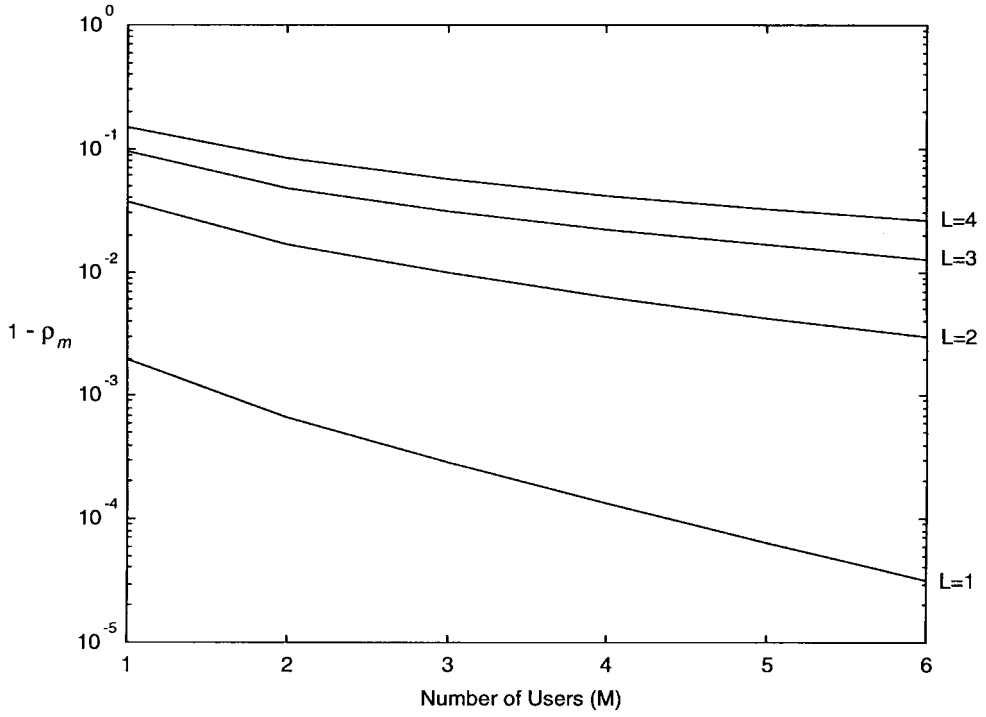

Fig. 9. Channel estimation accuracy required to achieve error floor of 10^{-3} with equipower users.

combining curves are not significantly affected since the error rate is approximately constant with SNR for $M > 2$.

Evidently, joint detection can support many more users than the number of antennas. This fact is clearly illustrated in Fig. 8 in which the error performance of both joint detection and MMSE combining are plotted against number of users at a fixed SNR of 12 dB. For this plot, $\rho_m = 0.99$ for all users—an appropriate value at 12 dB. As can be seen, the performance of joint detection degrades slowly and in a linear fashion as the number of users increases. In contrast, the performance of MMSE combining degrades very quickly and saturates at an unacceptably high error rate for $M > L$. For a large number of users, the performance of joint detection is orders of magnitude better than MMSE combining.

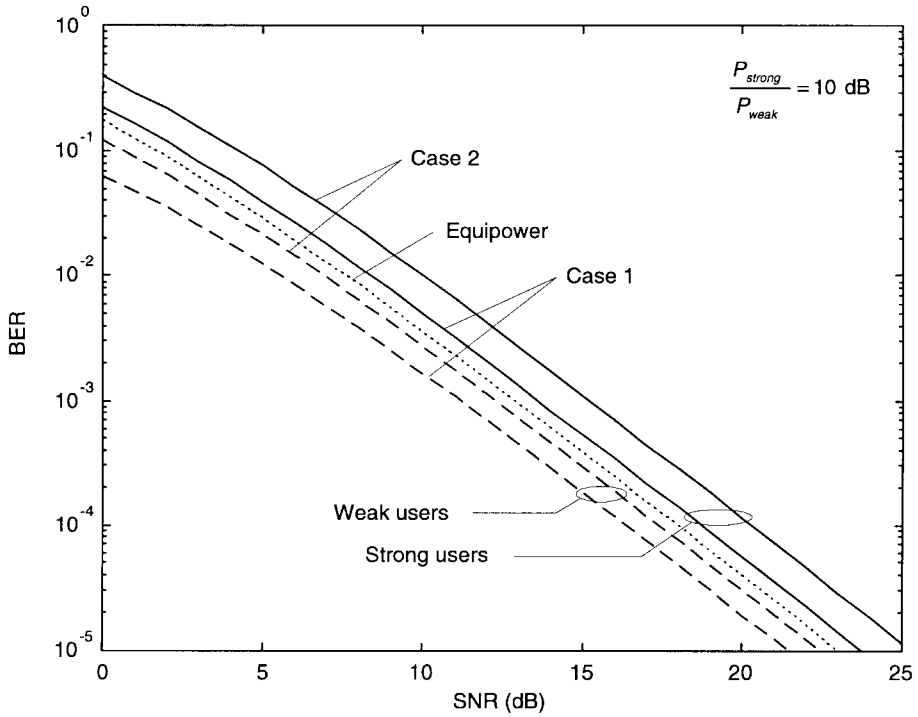

Fig. 10. Performance of joint detection of $M = 4$ nonequipower users with $L = 2$ antennas and perfect CSI. Case 1: three strong/one weak. Case 2: one strong/three weak.

To illustrate the channel estimation accuracy required to achieve a given performance for various numbers of equipower users and antennas, Fig. 9 shows the correlation coefficient ρ_m (same for all users) required to achieve an error floor of 10^{-3}. As can be seen, the accuracy requirements relax as each additional antenna is added. For example, for $L = 2$ antennas, the correlation coefficient must be no less than about 0.995 for the detection of $M = 4$ users. This results in a relative channel estimation error variance, defined as $\sigma^2_{e_m}/\sigma^2_{g_m}$, of approximately 1%. For $L = 4$ antennas, the correlation coefficient must be no less than about 0.95, resulting in a relative estimation error variance of approximately 10%.

C. Nonequipower Users

Thus far, the performance results presented have applied to the case of equipower users. It is interesting to investigate the nonequipower case to see how an unequal distribution of powers affects the performance of both the weak and strong users. Two different power distributions are examined, each for the detection of $M = 4$ users: case 1 corresponds to three strong users and one weak user; case 2 corresponds to one strong user and three weak users. The power difference between the weak and strong users in both cases is 10 dB.

Since the SNR for each user is different in the nonequipower case, a convention must be adopted for plotting the various users' performance. Accordingly, in the following graphs the BER of each user is plotted against its *own* SNR. The implication of this is that at a given SNR, the noise level (N_o) is different for each user: smaller for the weak users, larger for the strong users.

Fig. 10 shows the performance of cases 1 and 2 for perfect CSI compared to the case of equipower users. Due to the different noise levels at a given SNR, the performance of the weak users appears to be better than that of the strong users. To compare the performance at the same noise level, i.e., under the same operating conditions, one must mentally shift the weak users' curves to the right by an amount equivalent to the power difference between the users (10 dB in this case). Comparison under the same operating conditions reveals that the performance of the strong users is better than that of the weak users by about 7–8 dB. Moreover, the performance of all users is degraded from the equipower case, indicating that in an operational system some degree of power control may be desirable to keep the distribution of powers more or less uniform. Also evident from Fig. 10 is that the performance of case 1 is approximately 2 dB better for both strong and weak users than case 2, indicating that the larger the ratio of number of strong users to weak users, the better the performance.

For the case of imperfect CSI, the strong users are expected to have a larger ρ_m than the weak users, since, as mentioned in Section V-A, channel estimation accuracy typically improves with increasing SNR. The relative values are determined as follows. Using (9) and the fact that $\sigma^2_{e_m}$ varies inversely with Γ_m for PSAM, the correlation coefficient for one user (with SNR Γ_1) is related to that for a second user (with SNR Γ_2) by $|\rho_2| = \sqrt{1-(\Gamma_1/\Gamma_2)(1-|\rho_1|^2)}$. For example, if the strong users have $\rho_m = 0.999$ and the SNR difference is 10 dB, then the weak users have $\rho_m = 0.99$. Fig. 11 shows the performance of cases 1 and 2 using these values of ρ_m (fixed across the SNR range considered).

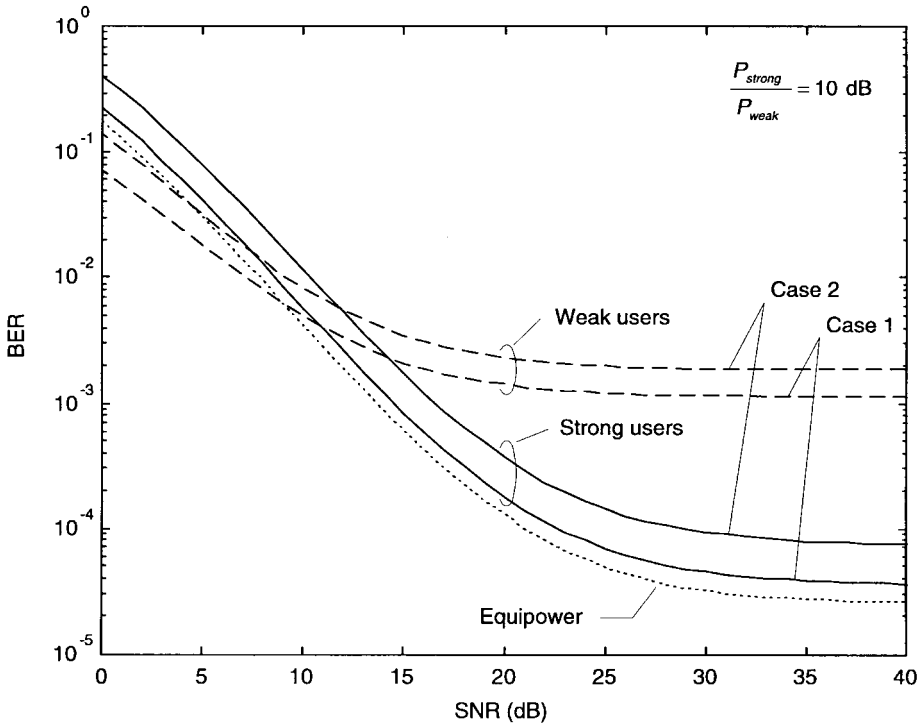

Fig. 11. Performance of joint detection of $M = 4$ nonequipower users with $L = 2$ antennas and imperfect CSI ($\rho_m = 0.999$ for strong users and 0.99 for weak users). Case 1: three strong/one weak. Case 2: one strong/three weak.

As before, to compare the performance of the weak and strong users at the same noise level, the weak users' curves must be shifted to the right by 10 dB. In contrast to case of perfect CSI, the difference in performance between the weak and strong users depends strongly on SNR. In the low-SNR region, where the effect of noise dominates that of channel estimation errors ($N_o \gg \sigma^2_{e_m}$), the difference is similar to the perfect CSI case. However, in the high-SNR region, where the effect of channel estimation errors dominates that of noise, the difference—due to the different ρ_m's—becomes much larger. Like before, if the more realistic variable ρ_m model is incorporated into the above, the curves become essentially parallel to those for the perfect CSI case, but shifted to the right by approximately 4 dB for both cases 1 and 2, and the error floor disappears.

VI. Conclusions

In this paper we have considered the joint detection of multiple cochannel symbol-synchronous PSK signals using a diversity antenna array in a system with channel estimates available at the receiver. A closed-form analytical expression has been derived, giving the union bound on error performance of the joint detection scheme, and is compared to the performance, obtained by simulation, of classical MMSE combining. The analysis applies to both perfect and imperfect channel estimation and is general in the sense that it is not focused on any particular channel estimation scheme.

The presented results show that the performance is very good: with joint detection it is possible to reliably detect multiple cochannel signals using only a single antenna. For perfect CSI, only a 2-dB penalty is incurred for each additional user. In the case of Q-ary PSK, the penalty is about 4.8 dB. For imperfect CSI, an error floor is introduced; however, within the limits of achievable channel estimation accuracy, it is shown that several users may still be supported while maintaining the error floor below 10^{-2}—a commonly accepted threshold value.

In the case of diversity reception, many more users than the number of antennas may be supported with a slow degradation in performance with each additional user. This contrasts sharply with the performance of classical MMSE combining which degrades quickly and saturates at an unacceptable level when the number of users equals and then exceeds the number of antennas. Furthermore, for all combinations of numbers of users and antennas, joint detection shows orders of magnitude improvement over MMSE combining.

The upper bound on BER for a single antenna and perfect CSI is compared with results from simulation and it is found to be asymptotically tight with increasing SNR. As the number of users increases, a given accuracy of the bound requires a somewhat higher SNR; however, the accuracy is quite satisfactory in the useful BER range.

Useful bounds are presented which indicate the channel estimation accuracy required in order to achieve a given level of performance for arbitrary numbers of users and antennas. Generally, the accuracy requirements of channel estimation relax significantly as the number of antennas is increased. These results should prove useful for those designing channel estimation schemes appropriate for multiuser receivers.

Unequal power distributions are investigated and it is found that both the weak and strong users' performance is degraded from the equipower case, indicating that in a practical system,

power control may be desirable. Furthermore, it is found that performance depends on the ratio of number of strong users to weak users and improves as this ratio increases.

APPENDIX
RANK OF $\mathbf{RF}_{ij}$

Here it is shown that the matrix $\mathbf{RF}_{ij}$ has only two nonzero eigenvalues, which allows the characteristic function of D_{ij} to be simplified from its form in (21b) to that in (22). First, recall that the dimension of both $\mathbf{R}$ and $\mathbf{F}_{ij}$ is $M+1$. Since the covariance matrix $\mathbf{R}$ is generally full rank, any limit on the rank of the product $\mathbf{RF}_{ij}$ is imposed by that of $\mathbf{F}_{ij}$. The rank of $\mathbf{F}_{ij}$ can be determined by looking at its null space, i.e., the solutions to the equation

$$\mathbf{F}_{ij}\mathbf{x} = \mathbf{0}. \tag{35}$$

Substituting (17) into this expression and rearranging gives

$$\mathbf{u}_i(\mathbf{u}_i^\dagger \mathbf{x}) - \mathbf{u}_j(\mathbf{u}_j^\dagger \mathbf{x}) = \mathbf{0}. \tag{36}$$

For $\mathbf{u}_i$ and $\mathbf{u}_j$ linearly independent, which is indeed the case for different $\mathbf{c}_i$ and $\mathbf{c}_j$, (36) is satisfied only for both $\mathbf{u}_i^\dagger \mathbf{x} = 0$ and $\mathbf{u}_j^\dagger \mathbf{x} = 0$. In other words, solutions to (36) lie in the $M-1$-dimensional subspace orthogonal to both $\mathbf{u}_i$ and $\mathbf{u}_j$. Since the nullity of $\mathbf{F}_{ij}$ is $M-1$ and the dimension of $\mathbf{F}_{ij}$ is $M+1$, the rank of $\mathbf{F}_{ij}$ is thus two. Consequently, the rank of the product $\mathbf{RF}_{ij}$ is a maximum of two for all M, implying that $\mathbf{RF}_{ij}$ has only two nonzero eigenvalues.

REFERENCES

[1] S. Verdu, "Minimum probability of error for asynchronous Gaussian multiple-access channels," *IEEE Trans. Inform. Theory*, vol. IT-32, pp. 85–96, Jan. 1986.

[2] R. Lupas and S. Verdu, "Linear multiuser detectors for synchronous code-division-multiple-access channels," *IEEE Trans. Inform. Theory*, vol. 35, pp. 123–136, Jan. 1989.

[3] P. Patel and J. Holtzman, "Analysis of a simple successive interference cancellation scheme in a DS/CDMA system," *IEEE J. Select. Areas Commun.*, vol. 12, pp. 796–807, June 1994.

[4] W. Van Etten, "Maximum likelihood receiver for multiple-channel transmission systems," *IEEE Trans. Commun.* vol. COM-24, pp. 276–283, Feb. 1976.

[5] K. Giridhar *et al.*, "Nonlinear techniques for the joint estimation of cochannel signals," *IEEE Trans. Commun.*, vol. 45, pp. 473–484, Apr. 1997.

[6] S. Gray, M. Kocic, and D. Brady, "Multiuser detection in mismatched multiple-access channels," *IEEE Trans. Commun.*, vol. 43, pp. 3080–3089, Dec. 1995.

[7] J. H. Winters, "Optimum combining in digital mobile radio with cochannel interference," *IEEE J. Select. Areas Commun.*, vol. SAC-2, pp. 528–539, July 1984.

[8] J. K. Cavers, "An analysis of pilot symbol assisted modulation for Rayleigh fading channels," *IEEE Trans. Veh. Technol.*, vol. 40, pp. 686–693, Nov. 1991.

[9] M. Schwartz, W. Bennett, and S. Stein, *Communications Systems and Techniques.* New York: McGraw-Hill, 1966.

[10] J. G. Proakis, *Digital Communications*, 2nd ed. New York: McGraw-Hill, 1989.

[11] R. A. Monzingo and T. W. Miller, *Introduction to Adaptive Arrays.* New York: Wiley, 1980.

Stephen J. Grant (S'94) was born in North Vancouver, B.C., Canada, in 1969. He received the B.A.Sc. degree from the University of British Columbia, Vancouver, B.C., Canada, in 1993, and the M.A.S.c. degree from Simon Fraser University, Burnaby, B.C., Canada, in 1996, both in electrical engineering. His M.A.Sc. thesis involved the analysis, design, and implementation of a DSP-controlled adaptive feedforward linearizer for RF power amplifiers. He is currently working toward the Ph.D. degree in electrical engineering at Simon Fraser University.

During 1993 and 1994 he was with MPR Teltech, Ltd., Burnaby, B.C., Canada, where he was involved with modem design for fixed wireless access systems. His research interests include multiuser detection and channel estimation techniques, adaptive antenna arrays, and integrated RF/DSP design for mobile communications.

James K. Cavers (M'90) received the B.A.Sc. degree in engineering physics and the Ph.D. degree in electrical engineering from the University of British Columbia, Vancouver, B.C., Canada, in 1966 and 1970, respectively.

From 1970 to 1979 he was with the Department of Systems Engineering, Carleton University, Ottawa, Ont., Canada, where he was first an Assistant Professor, and then an Associate Professor. From 1979 to 1982 he was with MacDonald Dettwiler and Associates, Vancouver, B.C., Canada, followed by a year with Glenayre Electronics, also in Vancouver, as a Senior Engineer. In 1983 he joined the School of Engineering Science, Simon Fraser University, Burnaby, B.C., Canada, as a Professor, and became Director of the School of Engineering Science from 1990 to 1994. His research interests include modulation and detection for mobile communications and integrated RF/DSP design.

Dr. Cavers received the Stentor Telecommunications Research Award in 1992 and the Gold Medal in Engineering and Applied Science from the Science Council of British Columbia in 1995.